

**Similarity renormalization, Hamiltonian flow equations, and Dyson's intermediate representation**

T. S. Walhout\*

*European Center for Theoretical Studies in Nuclear Physics and Related Areas, Villa Tambosi, Strada delle Tabarelle 286,  
I-38050 Villazzano (Trento), Italy*

(Received 17 June 1998; published 12 February 1999)

A general framework is presented for the renormalization of Hamiltonians via a similarity transformation. Divergences in the similarity flow equations may be handled with dimensional regularization in this approach, and the resulting effective Hamiltonian is finite since states well separated in energy are uncoupled. Specific schemes developed several years ago by Głazek and Wilson and by Wegner are shown to correspond to particular choices within this framework. A modification of Wegner's scheme is introduced with the idea of improving convergence. It is shown that a scheme for the transformation of Hamiltonians developed by Dyson in the early 1950s also arises from a particular choice within the similarity renormalization framework and is particularly suited to analytic computations since the usual counterterm structure used in Feynman perturbation theory is sufficient for this scheme. A logarithmically confining potential is shown to arise at second order in light-front QCD within Dyson's scheme, a result found previously for other similarity renormalization schemes that used sharp cutoffs in momentum space to regularize the Hamiltonian. Steps toward higher order and nonperturbative calculations are outlined. In particular, a set of equations analogous to Dyson-Schwinger equations is developed for both the Dyson scheme and the modified Wegner scheme. [S0556-2821(99)07204-5]

PACS number(s): 11.10.Gh; 11.10.Ef; 12.38.Aw

**I. INTRODUCTION**

While particle physics has been and remains to be guided by the desire to understand phenomena at ever shorter distances, one may nevertheless argue that the most vital challenge for quantum field theory has little to do with the physics at Planck length scales or a theory of everything (TOE). The challenge is how to solve strongly interacting quantum field theories, which inevitably amounts to understanding in a nonperturbative way how a theory designed to fit the physics of a smaller scale will determine the phenomena observed at greater length scales. The outstanding case is quantum chromodynamics (QCD), but the problem has existed since soon after the development of the renormalization program for quantum electrodynamics, when physicists began to study strongly interacting meson theories; and the problem must presumably be confronted by anyone who wants to show that any given TOE is indeed a TOE.

In ordinary quantum mechanics, strongly interacting systems may be handled by a variety of techniques based upon a Hamiltonian formulation of the theory in question. Relativistic quantum field theory, on the other hand, is studied almost exclusively in the Lagrangian formulation nowadays. Lagrangian methods are favored because they better allow one to keep symmetries of the theory manifest. However, this generally entails a sacrifice in calculational flexibility, with the result that one is limited to applications for which perturbative or semiclassical methods are valid (or at least hoped to be valid). This paper takes the view that a Hamiltonian formulation will provide a better starting point for the study of strongly interacting quantum field theories. It was this motivation, and the difficulties in its realization, that

eventually led Wilson [1] to formulate his version of the renormalization group, of which the similarity scheme used here is a specific example.

The renormalization group is most often used in a very restricted way in quantum field theory. Typically, renormalization is used as a tool only to cover up infinities, to select out well-behaved ("renormalizable") theories, and to make finite redefinitions of couplings so as to reorganize perturbative expansions in a better way. Renormalization transformations that produce more complicated interaction terms are generally avoided. This is because such transformations usually break at least some symmetries and complicate perturbative expansions. For a theory like QCD, however, perturbation theory is not powerful enough to calculate low-energy phenomena, for the lowest orders of a perturbative expansion look nothing like what one finds from low-energy experiments. In such a case, it might be worthwhile to consider a renormalization group transformation that brings new interactions, even if such a transformation hides symmetries that in the usual perturbative scheme remain manifest. The idea is that such a renormalization group transformation can be designed so that the new interactions it generates will contain the most important physics.

In fact, this is the main idea behind the similarity transformation of Hamiltonians.<sup>1</sup> The object of the similarity transformation is not primarily to produce a renormalized Hamiltonian, but rather to produce a Hamiltonian that can be dealt with in a way such that even first approximations in its

<sup>1</sup>Matrix elements of the transformed Hamiltonian  $H'$  are "similar" to the original Hamiltonian  $H$  if  $H' = PHP^{-1}$ . If  $H'$  is to be hermitian, we need  $P^\dagger = P^{-1}$ , and so the similarity transformations described here will all be unitary transformations.

\*Email address: walhout@ect.unitn.it

analysis provide a qualitatively correct description of the physics. That the similarity transformation can be used to renormalize a Hamiltonian that contains divergences is just a particular result of this more general requirement. The practical manifestation of this basic requirement is that the similarity transformation produces a Hamiltonian where only states of nearby energy contribute to phenomena at a given energy scale. Thus, Glazek and Wilson [2] introduced their similarity transformation to deal with divergences in light-front field theory, but also with the idea of using it to help transform the QCD Hamiltonian into a form for which a lowest-order approximation begins to look like a constituent quark model [3]. Wegner, [4] on the other hand, independently introduced a set of Hamiltonian flow equations to deal with many-body problems which have no need of the renormalization of divergences.

While our presentation of the similarity renormalization scheme roughly follows Ref. [3], we introduce certain generalizations that warrant a somewhat detailed summary of the framework. In particular, the adoption of the interaction picture is fundamental for what follows. The transformations of Wegner and of Glazek and Wilson are seen to follow from more specific choices within our formalism. These three authors are generally given credit for introducing the similarity transformation to field theory. Interestingly enough, however, soon after the development of renormalization theory, Dyson himself in a difficult, fascinating, and seemingly universally ignored series of papers [5] developed what he called the intermediate representation, which results from a transformation that matches all the requirements of the similarity transformations developed by Glazek, Wilson, and Wegner. This is of more than just historical interest [6]: we shall see that Dyson's scheme has some features that make it particularly suitable for perturbative calculations, and we shall adopt it in the following.

The outline of the paper is as follows. In the next section we provide a general interaction representation formulation of the similarity renormalization of Hamiltonians with respect to differences in unperturbed energies. We show how the schemes of Wilson and Glazek and of Wegner correspond to specific choices in our framework and introduce a modification to Wegner's scheme designed to improve convergence of the similarity flow equations. In Sec. III we discuss the perturbative solution of the similarity flow equations for these schemes by means of a diagrammatic expansion, which corresponds to that of old-fashioned time-ordered perturbation theory. This leads to a detailed discussion of Dyson's intermediate representation, which we show corresponds to a specific choice of perturbative scheme in the similarity renormalization framework.

The beauty of Dyson's scheme is that it may be represented diagrammatically in terms of generalized Feynman graphs—generalized in that amplitudes may be off energy shell. The difficulty comes in demonstrating this; we can only briefly summarize his scheme here, and we refer to his original papers for more details. We introduce a simple diagrammatic formulation of Dyson's scheme and show how it can be applied to light-front QCD (LFQCD) to great advantage. In particular, Dyson's scheme allows the use of dimen-

sional regularization and the Mandelstam-Leibbrandt prescription for the spurious light-front singularities, techniques unavailable to previous light-front similarity renormalization schemes. This leads to the main result of the paper: a second-order calculation of the quark-antiquark potential in LFQCD.

In Sec. IV we formulate the solution of the similarity flow equations in terms of general  $n$ -particle “dressed” vertices. The resulting equations, which look much like Dyson-Schwinger equations, are of second order in these vertices; and we show how a specific choice of similarity transformation—a modification of Wegner's scheme—can guarantee that these dressed vertices are joined by Feynman propagators, which therefore permits a Wick rotation to Euclidean space. We show how analogous equations can also be derived in Dyson's scheme and that these equations are linear in the dressed vertices. Finally, we give a specific example of how one may make approximations to sum a set of diagrams similar to those summed in the Bethe-Salpeter equation.

We shall refer to a generic theory of fermionic and vector bosonic fields throughout the paper. Only when we present the actual calculations do we specify our equations to the case of QCD in light-front coordinates and light-cone gauge. In Sec. III, we show that the similarity-transformed Hamiltonian contains a potential that rises logarithmically for large quark-antiquark separations, a result obtained previously in other similarity renormalization schemes [13–15]. This result is interesting because we employ a more popular regularization scheme than the previous calculations, which use sharp momentum-space cutoffs and a principle value prescription for the light-front infrared singularities—the latter of which is known to cause some difficulties [18]. We conclude that the confining potential is not dependent on the regularization scheme employed but is rather an inevitable consequence of the light-front similarity renormalization framework. In Sec. IV we discuss a ladder-type summation of these potentials. These examples are only meant to be suggestive. More detailed applications of our similarity renormalization framework will be undertaken in future papers.

Section V concludes the paper with a discussion of the ideas presented here. This last section is not just a summary, for it provides further motivation that could not properly be given before the scheme itself was developed. In particular, we discuss the significance of the similarity renormalization scheme for applications in light-front field theory and the motivation for the use of light-front coordinates in field theory in this light.

## II. SIMILARITY RENORMALIZATION SCHEME

### A. General formulation

We begin with a regularized field theoretical Hamiltonian  $H$ , derived in the usual way from a renormalizable relativistic Lagrangian. We write  $H = H_0 + H_{\text{int}}$ , with  $H_0$  the usual free Hamiltonian. Let us assume that  $H$  describes processes which at high energies may be well approximated by treating the interaction  $H_{\text{int}}$  perturbatively, but that its low-energy processes and its bound states are essentially nonperturba-

tive. The problem here is that  $H_0$  is a poor first approximation for calculating low-energy phenomena. The similarity renormalization scheme seeks to change the original Hamiltonian into a form that is more suitable for calculations over a wider range of energies. This is done by introducing an energy scale  $\sigma$  via a similarity transformation  $S_\sigma$  (which will always be unitary here). Roughly speaking, the transformed Hamiltonian  $H_\sigma = S_\sigma H S_\sigma^\dagger$  will depend on  $\sigma$ , the similarity scale, as follows: processes described by  $H$  which transfer an energy much greater than  $\sigma$  will be absorbed into the structure of  $H_\sigma$ , so that  $H_\sigma$  will only describe processes that correspond to energy transfers of order  $\sigma$  or less.

Thus, we call  $H$  the undressed Hamiltonian and  $H_\sigma$  the dressed Hamiltonian. The undressed Hamiltonian is renormalized; that is, the undressed Hamiltonian is the sum of a bare regularized Hamiltonian  $H_B$  and a set of counterterms  $H_C$  that removes any dependence in physical quantities upon the regulators. The structure of these counterterms must be determined as one solves for the dressed Hamiltonian  $H_\sigma$ . In particular, the counterterms in  $H$  ensure that  $H_\sigma$  will remain finite as the regulators are removed. The dressed Hamiltonian  $H_\sigma$  thus cannot produce infinities; and so the similarity transformation  $S_\sigma$  is finite, provided that it avoids singularities corresponding to small energy denominators. This latter restriction shall be discussed presently.

To define such a transformation, we write the unitary operator  $S_\sigma$  in terms of the anti-Hermitian generator of infinitesimal similarity scale transformations  $T_\sigma$ :

$$S_\sigma = \mathcal{S} \exp \left\{ \int_\sigma^\infty d\sigma' T_{\sigma'} \right\}, \quad (1)$$

where  $\mathcal{S}$  puts operators in order of increasing scale. Then the similarity transformation is given by the differential ‘‘flow’’ equation

$$\frac{dH_\sigma}{d\sigma} = -[T_\sigma, H_\sigma] \quad (2)$$

with the boundary condition  $H_\infty = H$ . Now let the eigenstates of  $H_0$  be  $|i\rangle$ , with  $H_0|i\rangle = E_i|i\rangle$ ; and write the matrix element of an operator  $\mathcal{O}$  as  $\mathcal{O}_{ij} = \langle i|\mathcal{O}|j\rangle$ . We wish to choose  $T_\sigma$  in such a way that

$$H_{\sigma ij} = f \left( \frac{E_i - E_j}{\sigma} \right) G_{\sigma ij}, \quad (3)$$

where the ‘‘similarity form factor’’  $f(x)$  is a smooth function such that

$$\begin{aligned} \text{(i)} \quad & f(0) = 1; \\ \text{(ii)} \quad & f(x) \rightarrow 0 \quad \text{as} \quad x \rightarrow \infty; \\ \text{(iii)} \quad & f^*(x) = f(-x); \end{aligned} \quad (4)$$

and  $G_\sigma$  is a finite Hermitian operator. The similarity function  $f$  has often been chosen to be a step function in previous work. However, this introduces nonanalyticities and in general should be avoided.

It is convenient to first write  $H_\sigma = H_0 + H_\sigma^{\text{int}}$  and transform to the interaction picture  $\mathcal{O}_I(t) = e^{iH_0 t} \mathcal{O} e^{-iH_0 t}$ , so that the ‘‘similarity flow’’ equation becomes

$$\frac{dH_{I\sigma}(t)}{d\sigma} = -i \frac{dT_{I\sigma}(t)}{dt} - [T_{I\sigma}(t), H_{I\sigma}(t)], \quad (5)$$

where  $H_{I\sigma}(t) = e^{iH_0 t} H_\sigma^{\text{int}} e^{-iH_0 t}$ —and so the undressed interaction Hamiltonian is  $H_I(t) = \lim_{\sigma \rightarrow \infty} H_{I\sigma}(t)$ . After Fourier transforming, Eqs. (3) and (5) become

$$H_{I\sigma}(\omega) = \sum_{ij} 2\pi \delta(\omega - E_i + E_j) H_{I\sigma ij} = f \left( \frac{\omega}{\sigma} \right) G_{I\sigma}(\omega) \quad (6)$$

and

$$\frac{dH_{I\sigma}(\omega)}{d\sigma} = \omega T_{I\sigma}(\omega) - \int \frac{d\omega'}{2\pi} [T_{I\sigma}(\omega'), H_{I\sigma}(\omega - \omega')], \quad (7)$$

respectively. Now we are ready to construct some suitable similarity operators  $T_\sigma(\omega)$ .

### B. Wilson’s and Głazek’s scheme

Wilson and Głazek first introduced similarity renormalization in the context of light-front Hamiltonian field theory [2]. Their transformation was later elaborated upon in Ref. [3]. Essentially, their choice of  $T_\sigma$  gives

$$T_{I\sigma}(\omega) = \frac{d}{d\sigma} \left\{ \frac{f \left( \frac{\omega}{\sigma} \right) - 1}{\omega f \left( \frac{\omega}{\sigma} \right)} H_{I\sigma}(\omega) \right\}, \quad (8)$$

which shall be called the WG scheme henceforth.<sup>2</sup> Note that property (4i) of  $f$  ensures that  $T_{I\sigma}(\omega)$  is finite as  $\omega \rightarrow 0$ , thereby avoiding possible problems with small energy denominators. This is a great advantage of the similarity renormalization scheme. The flow equation for the choice (8) is

$$\begin{aligned} H_{I\sigma}(\omega) = & f \left( \frac{\omega}{\sigma} \right) \left\{ H_I(\omega) \right. \\ & + \int_\sigma^\infty d\sigma' \int \frac{d\omega'}{2\pi} \left[ \frac{d}{d\sigma'} \left( \frac{f(\omega'/\sigma') - 1}{\omega' f(\omega'/\sigma')} H_{I\sigma'}(\omega') \right) \right. \\ & \left. \left. \times H_{I\sigma'}(\omega - \omega') \right] \right\}. \end{aligned} \quad (9)$$

The term  $d_{\sigma'} H_{I\sigma'}(\omega')$  on the right-hand side means that when we express this as a pure integral equation it will con-

<sup>2</sup>In the referred work the argument of  $f$  was  $(E_i - E_j)/(E_i + E_j + \sigma)$ . It is the modification to simple energy differences used here that makes the use of the interaction picture convenient.

tain terms of all orders in  $H_{I\sigma}$ . Presumably, this makes the equation rather difficult to solve.

### C. Wegner's scheme

Wegner introduced his Hamiltonian flow equation to study problems in condensed-matter physics [4]. In the present notation, his equation is

$$\frac{dH_\sigma}{d\sigma} = -\frac{1}{\sigma^3} [[H_0, H_\sigma], H_\sigma]. \quad (10)$$

This is a similarity transformation with the choice  $T_\sigma = [H_0, H_\sigma]/\sigma^3$ . Actually, Wegner advocates that  $H_0$  include not just the free Hamiltonian but also the number conserving part of the undressed—or even better, the dressed—interacting Hamiltonian. These are certainly choices which one can (and, perhaps, should) make in any similarity scheme, although they shall not be pursued further in this work.

Wegner's flow equation can be seen as resulting from a specific choice of the similarity function  $f$  in a more general scheme. This scheme, referred to hereafter as the W scheme, results from the following choice of the infinitesimal transformation operator:

$$T_{I\sigma}(\omega) = \frac{d}{d\sigma} \left\{ \frac{\ln f(\omega/\sigma)}{\omega} \right\} H_{I\sigma}(\omega), \quad (11)$$

which gives the following similarity flow equation:

$$H_{I\sigma}(\omega) = f\left(\frac{\omega}{\sigma}\right) \left\{ H_I(\omega) + \int_\sigma^\infty d\sigma' \int \frac{d\omega'}{2\pi} \frac{d\sigma'}{\omega' f(\omega'/\sigma')} \right. \\ \left. \times [H_{I\sigma'}(\omega'), H_{I\sigma'}(\omega - \omega')] \right\}. \quad (12)$$

This closed integral equation looks simpler than Eq. (9), although it is still nonlinear in the dressed Hamiltonian. To recover Wegner's flow equation one just chooses  $f(x) = e^{-(1/2)x^2}$ , which fulfills all the requirements Eq. (4) of a similarity function. Using Eq. (6), the flow equation (12) becomes

$$G_{I\sigma}(\omega) = H_I(\omega) - \int_\sigma^\infty \frac{d\sigma'}{\sigma'^2} \int \frac{d\omega'}{2\pi} F\left(\frac{\omega+2\omega'}{2\sigma'}, \frac{\omega-2\omega'}{2\sigma'}\right) \\ \times \left[ G_{I\sigma'}\left(\frac{1}{2}\omega + \omega'\right), G_{I\sigma'}\left(\frac{1}{2}\omega - \omega'\right) \right], \quad (13)$$

where

$$F(x_1, x_2) = -\frac{f(x_1)f'(x_2)}{f(x_1+x_2)}. \quad (14)$$

With Wegner's choice of  $f$ , the form factor in Eq. (13) is  $F_{\sigma'} = (\omega/2\sigma' + \omega'/\sigma') e^{\omega^2/4\sigma'^2} e^{-\omega'^2/\sigma'^2}$ ; and the divergent dependence on  $\omega$ , while tamed by the overall factor  $f(\omega/\sigma)$  in Eq. (12), will nevertheless favor higher orders in an iterative solution of  $H_{I\sigma}(\omega)$ .

We suggest that a similarity function  $f(x)$  that falls off less sharply—for example, of the form  $(1+x^2)^{-m}$ , which goes as  $x^{-2m}$  when  $x \rightarrow \infty$ —might be preferred over Wegner's choice. In particular, for  $m=1$  this latter choice gives

$$F\left(\frac{\omega+2\omega'}{2\sigma'}, \frac{\omega-2\omega'}{2\sigma'}\right) \\ = \frac{\sigma'^3(\omega+2\omega')(\sigma'^2+\omega^2)}{[\sigma'^2+(\omega/2-\omega')^2][\sigma'^2+(\omega/2+\omega')^2]^2}, \quad (15)$$

which falls off as  $\omega^{-3}$  when  $\omega \rightarrow \infty$ . This damps far-off-diagonal contributions to  $G_{I\sigma}(\omega)$  that come from the nonlinear term in Eq. (13). This choice is also convenient for the development of Dyson-Schwinger-like equations in Sec. IV.

## III. PERTURBATIVE SOLUTION OF FLOW EQUATIONS

### A. In the WG and W schemes

One may look for solutions to the similarity flow equations by expanding in the undressed interaction  $H_I(\omega)$  via

$$G_{I\sigma}(\omega) = \sum_{n=1}^{\infty} \int \frac{d\omega_1}{2\pi} \cdots \int \frac{d\omega_n}{2\pi} g_{\sigma\omega}^{(n)} 2\pi \\ \times \delta(\omega - \omega_1 - \cdots - \omega_n) H_I(\omega_1) \cdots H_I(\omega_n). \quad (16)$$

Then the functions  $g_{\sigma\omega}^{(n)} \equiv g_\sigma^{(n)}(\omega_1, \dots, \omega_n)$ ,  $n \geq 2$ , satisfy the recursion equation

$$g_{\sigma\omega}^{(n)} = \sum_{m=1}^{n-1} \int_\sigma^\infty \frac{d\sigma'}{\sigma'^2} \{ F(\Omega_n - \Omega_m, \Omega_m) \\ - F(\Omega_m, \Omega_n - \Omega_m) \} g_{\sigma'\omega}^{(m)} g_{\sigma'\omega}^{(n-m)}, \quad (17)$$

for the W scheme, with  $g_\sigma^{(1)} = 1$ . We have defined here  $\Omega_k = (\omega_1 + \cdots + \omega_k)/\sigma'$ . A somewhat more complicated equation can also be determined for the WG scheme.

The similarity transformed Hamiltonian is then obtained by normal ordering the field operators in the right-hand side of Eq. (16), giving a unique representation in terms of normal-ordered products of field operators:

$$G_{I\sigma}(\omega) = \sum_{\mathcal{N}} g_{\sigma\mathcal{N}}(\{p\}, \omega) \mathcal{N}_{\{p\}}, \quad (18)$$

where the sum includes integrals over the momenta  $p_i$  associated with the fermion and boson creation and destruction operators in the normal-ordered product  $\mathcal{N}_{\{p\}}$ . A given normal-ordered term with coefficient  $g_{\sigma\mathcal{N}}$  in the dressed Hamiltonian will have contributions from an infinite number of terms in expansion (16), with each contribution consisting of an integration over the product of  $g_\sigma^{(n)}$  with one or more functions coming from the contractions of the field operators in Eq. (16). Since these contractions do not come from time-ordered products, one has many more contraction terms than

in Feynman perturbation theory. Indeed, the resulting diagrammatic expansion [3] is that of old-fashioned perturbation theory.

### B. Dyson's scheme

If the scale  $\sigma$  is large enough, then it is reasonable to solve the similarity flow equations perturbatively as above; for then only high-energy processes will dress  $H_{I\sigma}$ , and we have assumed for our theory that the interactions governing such processes are weak. However, the proliferation of diagrams in old-fashioned perturbation theory makes the above schemes quite tedious. Even second-order calculations can be rough; and in light-front field theory, where similarity renormalization methods have been in use for several years now, little has been accomplished at higher orders. Thus it is more than a curiosity that Dyson long ago developed a similarity renormalization scheme that is based upon the evaluation of off-energy-shell Feynman diagrams. Dyson's intermediate representation was developed over several long papers, and we refer the interested reader to the original work [5] for more details. Here we just summarize the salient features in showing how Dyson's scheme fits into our similarity renormalization framework.

Dyson considered the transformation  $\mathcal{O}_D(t) = S_D^{-1}(t)\mathcal{O}_I(t)S_D(t)$  of interaction representation operators to another representation induced by the unitary operator

$$S_D(t) = \mathcal{T}\{e^{-i\int_{-\infty}^t dt' H_I(t,t')}\}, \quad (19)$$

where  $\mathcal{T}$  is the usual time-ordering operator (acting only on the integrated times in the expansion of the exponential) and  $H_I(t,t')$  is obtained from  $H_I(t')$  by rescaling each occurrence of the renormalized coupling  $g_R$  in  $H_I(t')$ , including the counterterms, via  $g_R \rightarrow \tilde{f}(\sigma(t-t'))g_R$ , with  $\tilde{f}(t-t') \rightarrow 0$  as  $t' \rightarrow -\infty$  and  $\tilde{f}(0) = 1$ . We write

$$H_I(t,t') = \sum_{n=1}^{\infty} [g_R \tilde{f}(\sigma(t-t'))]^n \int d^3x' \mathcal{H}_I^{(n)}(x'). \quad (20)$$

Note that as the energy scale  $\sigma \rightarrow 0$ ,  $\tilde{f} \rightarrow 1$ ; and so in this limit  $S_D(t)$  becomes the familiar time-evolution operator that transforms from the Heisenberg to the interaction pictures. In this limit, then, we can think of the ‘‘bare’’ interaction-picture operators as being dressed adiabatically with interactions by Dyson's transformation.

For finite  $\sigma$ , however, only some of the interactions are put into the operators; and so  $S_D^{-1}(t)$  then transforms to an

intermediate representation, which we have labeled with a  $D$  (Dyson picture). In particular, the intermediate Hamiltonian is  $H_D(t) = S_D^{-1}(t)H(t)S_D(t)$ ; and under this transformation low-energy processes, corresponding to large times  $T \gg 1/\sigma$ , do not modify  $H_D(t)$  whereas high-energy processes do. As a result, the intermediate Hamiltonian suppresses processes corresponding to large energy differences between asymptotic states. Indeed, Dyson chose the form

$$\tilde{f}(\sigma t) = \int_0^{\infty} d\Gamma f(\Gamma) e^{-\Gamma \sigma t} \quad (21)$$

(so  $\tilde{f}$  is the Laplace transform of  $f$ ) and showed that if one imposes the condition  $\tilde{f}'(0) = 0$  then the (Fourier-transformed) intermediate representation Hamiltonian obeys

$$H_D(\omega) \propto \frac{1}{\omega^2} \quad \text{as } \omega \rightarrow \infty. \quad (22)$$

Moreover, we can identify the infinitesimal similarity transformation operator associated with  $S_D(t)$  as

$$\begin{aligned} T_D(t) &= S_D^{-1}(t) \frac{d}{d\sigma} S_D(t) \\ &= - \sum_{n=1}^{\infty} i^n \int_{-\infty}^t dt_1 \cdots \int_{-\infty}^{t_{n-1}} dt_n [H_I(t,t_n), \dots \\ &\quad \times [H_I(t,t_2), d_{\sigma} H_I(t,t_1)] \dots]. \end{aligned} \quad (23)$$

Thus Dyson's transformation is an explicit perturbative representation of a similarity transformation, and the label  $D$  will always imply a  $\sigma$  scale dependence.

Writing  $H_D(t) = H_0 + H_I^D(t)$  and using Dyson's parametrization (21), the intermediate Hamiltonian may be expressed as a sum over normal-ordered products of field operators

$$\begin{aligned} H_I^D(\omega) &= \sum_{n=1}^{\infty} (g_R)^n \left\{ \prod_{i=1}^n \int_0^{\infty} d\Gamma_i f(\Gamma_i) \right\} \sum_{\mathcal{N}} \\ &\quad \times \mathcal{M}_{\mathcal{N}}^{(n)}(\omega, \{p\}, \{\Gamma\}) \mathcal{N}_{\{p\}}. \end{aligned} \quad (24)$$

The  $\mathcal{M}_{\mathcal{N}}^{(n)}$  are c-number amplitudes depending on the field-operator momenta  $p_i$  and the ‘‘damping’’ factors  $\Gamma_k$ . In the following, the integrals in the brackets in Eq. (24) shall be included implicitly in sum over  $n$ . Dyson showed that the amplitudes  $\mathcal{M}$  can be calculated after analytic continuation from the expression

$$\begin{aligned} \sum_{\mathcal{N}} \mathcal{M}_{\mathcal{N}}^{(n)} \mathcal{N} &= \sum_{m=0}^{\infty} \frac{(-i)^m}{m!} \sum_{\{n_m\}} \sigma n_0 \Gamma_1 \left\{ \prod_{i=0}^m \int d^4x_i \right\} \int_{-\infty}^{\infty} dt \theta(t-t_0) \\ &\quad \times e^{-i(\omega - \sigma \Gamma_1 - \dots - \sigma \Gamma_m)t} \mathcal{T}\{\mathcal{H}_{\Pi}^{(n_0)}(x_0) \cdots \mathcal{H}_{\Gamma}^{(n_m)}(x_m)\}, \end{aligned} \quad (25)$$

where the second sum on the right is restricted such that  $\sum_i n_i = n$  and using Eq. (20) we have defined the ‘‘damped’’ Hamiltonian density

$$\mathcal{H}_{I\Gamma}^{(n_i)}(x_i) = \exp\left(\sum_{k=n_{i-1}+1}^{n_i} \Gamma_k \lambda \cdot x_i\right) \mathcal{H}_I^{(n_i)}(x_i). \quad (26)$$

We have also defined for future convenience the four-vector  $\lambda_\mu = \sigma n_\mu$ , where  $n^2 = 1$  and  $n \cdot x = x^0$ . In evaluating Eq. (25), the  $\Gamma_k$  are to be considered pure imaginary numbers. Then the calculation of the amplitudes  $\mathcal{M}$  amounts essentially to the evaluation of ordinary Feynman graphs. The only difference is that energy conservation at each vertex  $x_i$  is spoiled by a factor  $i(\Gamma_{n_{i-1}+1} + \dots + \Gamma_{n_i})$ , and so one needs to introduce a new graphical element.

### C. Doubled Feynman graphs and spurions

Dyson described a graphical method, using what he called ‘‘doubled’’ Feynman diagrams, for calculating intermediate representation operators from expressions such as Eq. (25). A doubled Feynman diagram is an ordinary connected  $m + 1$ -point Feynman graph in which a simply connected ‘‘tree’’ of (fermion and/or boson) propagator lines are drawn double. An example is given in Fig. 1. The doubled lines account for the damping factors  $\Gamma_k$ . The rules for the evaluation of such diagrams may be found in [5].

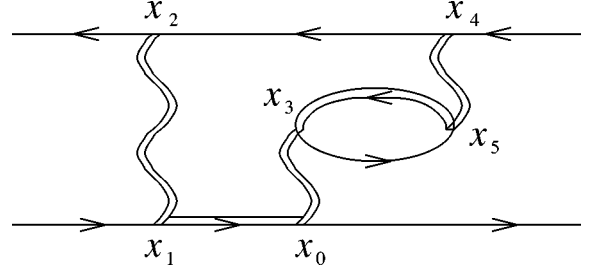


FIG. 1. Doubled Feynman graph.

We instead introduce here an alternate but entirely equivalent (and hopefully more transparent) diagrammatic scheme that borrows from a formulation of perturbation theory due to Kadyshevsky [7,8]. To do this, we express the step function in Eq. (25) as a complex integration through the familiar representation

$$\theta(t-t_0) = \int \frac{d\nu}{2\pi i} \frac{e^{i\nu(t-t_0)}}{\nu - i\varepsilon} = \int \frac{d\nu}{2\pi i} \frac{e^{i\nu\sigma(t-t_0)}}{\nu - i\varepsilon}. \quad (27)$$

Then from Eqs. (24) and (25), we find the Fourier transform of the interaction part of the total intermediate representation momentum is

$$\begin{aligned} \mathcal{P}_{I\mu}^D(p) &= n_\mu H_I^D(p) \\ &= \lambda_\mu \sum_{n=1}^{\infty} g_R^n \sum_{m=0}^{\infty} \frac{(-i)^m}{m!} \int \frac{d\nu}{2\pi} \frac{-\Lambda_0}{\nu - i\varepsilon} \sum_{\{n_i\}} \int d^4x e^{-i(p - \Lambda_m + \Lambda) \cdot x} \\ &\quad \times \left\{ \prod_{i=0}^n \int d^4x_i \right\} e^{-i(\Lambda_0 - \Lambda) \cdot x_0} e^{-i(\Lambda_1 - \Lambda_0) \cdot x_1} \dots e^{-i(\Lambda_{m-1} - \Lambda_m) \cdot x_m} \mathcal{T}\{\mathcal{H}_I^{(n_0)}(x_0) \mathcal{H}_I^{(n_1)}(x_1) \dots \mathcal{H}_I^{(n_m)}(x_m)\}, \end{aligned} \quad (28)$$

where  $\Lambda_i^\mu \equiv i(\Gamma_1 + \dots + \Gamma_{n_i})\lambda^\mu$  and  $\Lambda^\mu = -\nu\lambda^\mu$ . We expand the time-ordered product in terms of operator products  $\mathcal{N}$  and perform the configuration space integrals in Eq. (28), so that the amplitudes  $\mathcal{M}_{\mathcal{N}}^{(m,n)}$  result from integrations of  $l \geq m - 1$  Feynman propagators depending on  $l$  internal momenta  $q_k$ . Shifting the space-time variables in Eq. (28) as  $x_i \rightarrow x_i + x$ , we see that  $\mathcal{M}$  is multiplied by an overall  $\delta$  function

$$\mathcal{M}_{\mathcal{N}}^{(m,n)}(\{p\}, \{\Gamma_{ij}\}, \nu) \propto (2\pi)^4 \delta^{(4)}(p - p^O + p^I), \quad (29)$$

which arises from integration over  $x$ . Here  $p^O$  is the sum of outgoing and  $p^I$  the sum of ingoing external momenta. The remaining integrals over the  $x_i$  give the  $\delta$  functions:

$$(2\pi)^4 \delta^{(4)}(p_i^O - p_i^I + q_i^O - q_i^I - \Lambda_i + \Lambda_{i-1}), \quad (30)$$

where  $p_i^O$  is sum of the external momenta leaving  $x_i$ ,  $q_i^I$  is the sum of the internal momenta entering  $x_i$ , and so forth.

Thus the amplitudes  $\mathcal{M}_{\mathcal{N}}^{(m,n)}$  are connected  $m + 1$ -point Feynman diagrams whose dependence upon the  $\Lambda_i$  may be accounted for by drawing an additional directed dashed line

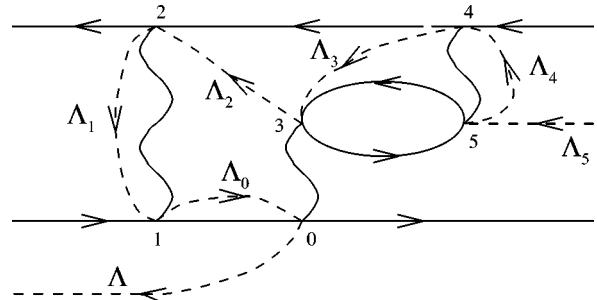


FIG. 2. Spurion graph corresponding to Fig. 1.

as in Fig. 2, which is equivalent to Fig. 1. This is very similar to the spurion line of Kadyshevsky's diagrammatic scheme [7]. Although the rules for our scheme are quite different than those of Kadyshevsky's, we shall still call our dashed line a spurion line. We treat the variables  $\Lambda^\mu$  and  $\Lambda_i^\mu$  as momenta and stipulate that the spurion line carries momentum as shown in Fig. 2—namely, the spurion line entering vertex  $i$  has momentum  $\Lambda_i$ , and that exiting vertex 0 has momentum  $\Lambda$ . The spurion line touches each vertex exactly once, proceeding in decreasing order from vertex  $m$  to 0. A relabeling of the vertices 1 through  $m$  will not produce a distinct diagram since Eq. (28) is symmetric with respect to  $\Gamma_i \leftrightarrow \Gamma_j, i \neq j \neq 0$ , and so for a given choice of vertex 0 we may choose any ordering of 1 through  $m$  and ignore all others, for they just sum to cancel the factor  $1/m!$  in Eq. (28). As in the scheme of Kadyshevsky, we may think of the spurion line as ordering the different vertices in time; however, it is only the order of vertex 0 that need be distinguished from that of the others.

With the spurion line considered as carrying momentum in the way described above, we have the usual four-momentum conservation at each vertex; and the evaluation of the amplitude  $\mathcal{M}$  proceeds as that of an ordinary Feynman graph. The spurion line serves only to shift the internal momenta so that the dependence on the  $\Lambda_i$  is now carried by the Feynman propagators—this is precisely the role of the doubled lines in Dyson's formulation. There will also always be an overall  $\delta$  function of the form  $\delta^{(4)}(p - \Lambda_m + \Lambda)$ , which expresses conservation of total three-momentum but not energy. The dependence of  $\mathcal{M}$  upon the variables  $\Gamma_1$  and  $\nu$  comes solely from this latter  $\delta$  function, and so the integrals over these variables in Eq. (28) will yield the similarity function described earlier, a function that by choice of  $f(\Gamma_1)$  falls off at least as rapidly as  $1/\omega^2$  when the total-energy difference  $\omega = p^0$  diverges.

An important advantage of Dyson's scheme is the apparent invariance of the expression (28). The  $\Gamma_i$  and  $\nu$  are dimensionless scalars, and covariance is broken only by  $\lambda = \sigma n$ , which was chosen to have a special form. We note now that the choice  $n = (1, 0, 0, 0)$  above gives the equal-time formulation described here, but one could just as well choose  $n = n_+$  with  $n_+^2 = 0$ ,  $n_+ \cdot x = x^+ = x^0 + x^3$ . This latter choice of  $\lambda$  ensures that Eq. (28) yields the light-front formulation of the Hamiltonian, with  $x^+$  the "light-front time." It is important, however, that divergences arising from the integrations in Eq. (28) are independent of  $\lambda$ , for they occur when the internal momenta of our Feynman graphs diverge with respect to the variables  $\Lambda_i$ . Thus the determination of the counterterm structure of  $H_I$  is entirely equivalent to ordinary Feynman perturbation theory.<sup>3</sup> In particular, the usual rules for power counting, separation of divergences and mul-

<sup>3</sup>As with Feynman perturbation theory, the light-cone gauge choice  $A^+ = n_+ \cdot A = 0$  is noncovariant and necessitates the introduction of counterterms [11] that depend on  $n_\pm = (1, 0, 0, \pm 1)$ . Such counterterms, of course, cannot depend on  $\sigma$ .

tiplicative renormalizability apply, results that are by no means clear in other schemes for light-front variables.

#### D. LQCD $q\bar{q}$ potential

As an example we shall look at the quark-antiquark potential in light-front QCD. We do not discuss at length any of the many interesting, enticing, and puzzling features of light-front QCD. For more details see Refs. [3] and [15]. Here we only highlight those features relevant to our calculation and postpone any further discussion to the final section.

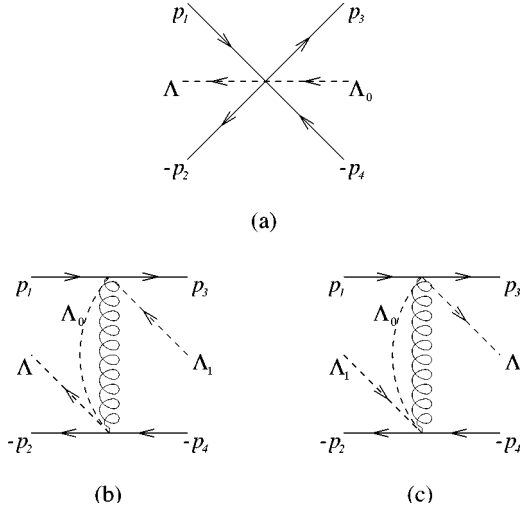
When formulated using light-front variables<sup>4</sup> and light-cone gauge, half the degrees of freedom of QCD are constrained and one may develop an effective theory in which the gluons and quarks are two-component fields [9]. For some calculations it is more appropriate to use the original four-component constrained theory [10,11]—for example, to demonstrate that the Slavnov-Taylor identities are fulfilled [12,11]. In general, however, calculations are simpler in the two-component theory, and we use this theory here. The Feynman rules for the two-component effective theory may be found in the appendix of Ref. [9]. We calculate the coefficient of the  $q\bar{q} \rightarrow q\bar{q}$  term in the intermediate Hamiltonian to second order in the undressed coupling  $g_R$ . Perry [13] first showed using a discrete similarity transformation (with the similarity function  $f$  chosen to be a step function) that one obtains a logarithmically confining potential in the dressed Hamiltonian. Zhang [14] later showed that a continuous similarity transformation such as those described here (specifically, the WG scheme of Ref. [3] with  $f$  a step function) yields a potential of the same form. Wilson and Robertson [16] gave general arguments (and caveats) for the appearance of such a confining potential in similarity transformed light-front QCD Hamiltonians. Głazek [15] also gives a detailed discussion and derivation of the potential. Here, we show how such a potential arises within Dyson's scheme.

The graphs that contribute at second order are shown in Fig. 3. Graph 3(a) comes from a term  $g_R^2 \mathcal{H}_I^{(2)}(x)$  in the undressed Hamiltonian that arises from eliminating the constrained components of the gluon field [9]. The amplitudes corresponding to the graphs in Fig. 3 are

$$i\mathcal{M}_a = -4ig_R^2 T^a T^a \frac{1}{[p_1^+ - p_3^+]^2} (2\pi)^4 \delta^{(4)}(p - \Lambda_0 + \Lambda), \quad (31)$$

where  $p = p_3 + p_4 - p_2 - p_1$  and  $\Lambda_0 = i\lambda(\Gamma_1 + \Gamma_2)$ ;

<sup>4</sup>Light-front longitudinal momentum is  $p^+ = n_+ \cdot p = p^0 + p^3$ , light-front energy is  $p^- = n_- \cdot p = p^0 - p^3$ , and transverse momentum is  $p_\perp^i = p^i$ ,  $i = 1, 2$ . The scalar product is  $p \cdot x = \frac{1}{2}p^+x^- + \frac{1}{2}p^-x^+ - p_\perp \cdot x_\perp$ , where the notation  $p_\perp \cdot x_\perp$  means  $p^1x^1 + p^2x^2$ . Occasionally, it is convenient to define the light-front 3-vector  $\bar{p} = (p^+, p_\perp)$  and the product  $\bar{p} \cdot \bar{x} = p^+x^- - p_\perp \cdot x_\perp$ . On-shell particles satisfy  $p^- = (p_\perp^2 + m^2)/p^+$ , from which it follows that transverse momenta scale as masses but longitudinal momenta scale differently.

FIG. 3. Order  $g_R^2$  diagrams contributing to  $q\bar{q} \rightarrow q\bar{q}$ .

$$\begin{aligned}
 i\mathcal{M}_b = & \left\{ \frac{q_\perp^i}{[q^+]} - \frac{\sigma_\perp \cdot p_{3\perp} - im}{2[p_3^+]} \sigma_\perp^i - \sigma_\perp^i - \sigma_\perp^i \frac{\sigma_\perp \cdot p_{1\perp} + im}{2[p_1^+]} \right\} \\
 & \times \frac{-4ig_B^2 T^a T^a}{q^2 + i\epsilon} \left\{ \frac{q_\perp^i}{[q^+]} - \frac{\sigma_\perp \cdot p_{2\perp} - im}{2[p_2^+]} \sigma_\perp^i \right. \\
 & \left. - \sigma_\perp^i \frac{\sigma_\perp \cdot p_{4\perp} + im}{2[p_4^+]} \right\} (2\pi)^4 \delta^{(4)}(p - \Lambda_1 + \Lambda), \quad (32)
 \end{aligned}$$

$$\begin{aligned}
 iV_{LR} \delta^{(3)}(\bar{p}) = & -4g_R^2 T^a T^a \delta^{(3)}(\bar{p}) \int_0^\infty d\Gamma_1 f(\Gamma_1) \int_0^\infty d\Gamma_2 f(\Gamma_2) \frac{\sigma \Gamma_1}{p^- - i\sigma(\Gamma_1 + \Gamma_2)} \\
 & \times \left\{ \frac{(q^-)^2}{(q^+ q^- + i\epsilon)^2} \cdot \frac{q^+ q^-}{q^+ q^- - q_\perp^2 + i\epsilon} + \frac{(\bar{q}^-)^2}{(q^+ \bar{q}^- + i\epsilon)^2} \cdot \frac{q^+ \bar{q}^-}{q^+ \bar{q}^- - q_\perp^2 + i\epsilon} \right\}, \quad (35)
 \end{aligned}$$

where  $q^- = p_3^- - p_1^- - i\sigma\Gamma_2$  and  $\bar{q}^- = p_2^- - p_4^- + i\sigma\Gamma_2$ . For small  $\bar{q} = \bar{p}_3 - \bar{p}_1 = \bar{p}_2 - \bar{p}_4$ , the energy difference  $p^-$  can be ignored with respect to  $\sigma$ . We calculate  $V_{LR}(x^-, x_\perp)$ , the Fourier transform with respect to  $\bar{q}$  of Eq. (35) under this approximation. We need to be careful, however, for  $V_{LR}(0,0)$  diverges. This is a result of well-known infrared singularities due to the choice of light-cone gauge, singularities that are known to cancel (in perturbation theory, at least) when evaluating gauge invariant quantities.

Now, when using light-front variables, we need to take into account that transverse and longitudinal variables scale differently. Thus there is a transverse mass scale  $\mu$  and a longitudinal momentum scale  $\rho$ . The energy scale is then  $\sigma = \mu^2/\rho$ . It is natural to use dimensional regularization to handle both ultraviolet and infrared divergences in our scheme by taking the number of transverse dimensions to be  $d$  instead of 2. Then we must introduce an arbitrary (transverse) mass scale, which we take to be  $\mu$ . This means the similarity flow is governed by the longitudinal scale  $\rho$ . That

where  $p$  is as above,  $\Lambda_0 = i\lambda\Gamma_1$ ,  $\Lambda_1 = i\lambda\Gamma_2 + \Lambda_0$ , and  $q = p_3 - p_1 + \Lambda_0 - \Lambda_1$ ; and, finally,  $\mathcal{M}_c$  is obtained from  $\mathcal{M}_b$  by the substitutions  $\Lambda \leftrightarrow -\Lambda_1$ , and  $\Lambda_0 \rightarrow -\Lambda_0$ . In general, we need to regulate the singularities as the longitudinal momentum  $q^+ = n \cdot q \rightarrow 0$ . As is usual for Feynman diagrams in light-front variables, we use the Mandelstam-Leibbrandt prescription [17]

$$\frac{1}{[q^+]} = \frac{q^-}{q^+ q^- + i\epsilon} = \frac{1}{q^+ + i\epsilon \Re(q^-)}. \quad (33)$$

For the four-point interaction of Eq. (31), we interpret this prescription to be

$$\begin{aligned}
 \frac{2}{[p_1^+ - p_3^+]^2} \rightarrow & \left\{ \frac{p_1^- - p_3^-}{(p_1^+ - p_3^+)(p_1^- - p_3^-) + i\epsilon} \right\}^2 \\
 & + \left\{ \frac{p_4^- - p_2^-}{(p_1^+ - p_3^+)(p_4^- - p_2^-) + i\epsilon} \right\}^2. \quad (34)
 \end{aligned}$$

The potential  $V(p_1, p_2, p_3, p_4)$  is proportional to the sum of these terms,  $\mathcal{M}_a + \mathcal{M}_b + \mathcal{M}_c$  integrated over the variables  $\Gamma_i$ . We are interested in how this potential behaves at large separations, for which the terms proportional to  $[q^+]^{-1}$  will dominate the expressions in the brackets in Eq. (32). Summing the three diagrams, we have then for the long-range part of the potential

the couplings now run with two scales will have profound implications at higher orders, but this does not concern us at present. Setting  $p^- \rightarrow 0$  in Eq. (35), generalizing to  $d$  transverse dimensions and taking the Fourier transform, we find

$$\begin{aligned}
 V_{LR}(x^-, x_\perp) = & \frac{g_R^2 \mu^2}{4\pi\rho} T^a T^a \\
 & \times \int_0^\infty d\Gamma_1 f(\Gamma_1) \int_0^\infty d\Gamma_2 f(\Gamma_2) \frac{4\Gamma_1 \Gamma_2}{\Gamma_1 + \Gamma_2} \\
 & \times \left\{ \frac{2}{2-d} + \gamma + E_1 \left( \Gamma_2 \frac{\mu^2 x_\perp^2}{4\rho|x^-|} \right) \right. \\
 & \left. + \ln \left( \frac{\mu^2 x_\perp^2}{4\pi} \right) \right\}, \quad (36)
 \end{aligned}$$

where  $\gamma$  is the Euler-Mascheroni constant and  $E_1(x) = -Ei(-x)$  is the exponential integral function. This gives

a long-range logarithmic potential independent of the choice of  $f(\Gamma)$ , which just affects its strength. Indeed, we can use the relation  $E_1(z) \rightarrow -\gamma - \ln z$  for  $z$  small to see that

$$V_{LR} \sim \ln \rho |x^-| \quad \text{for} \quad 4\rho |x^-| \gg \Gamma_2 \mu^2 x_\perp^2; \quad (37)$$

otherwise,  $E_1$  is of order 1 and the  $\ln \mu^2 x_\perp^2$  term dominates.

$$V_{SR}(x_\perp) = \frac{g_R^2 \mu^2 T^a T^a}{4\pi\rho} \int_0^\infty d\Gamma_1 \int_0^\infty d\Gamma_2 \frac{2\Gamma_1 f(\Gamma_1) \Gamma_2 f(\Gamma_2)}{\Gamma_1 + \Gamma_2} \left\{ -i \cos^{-1}(\hat{x}_\perp \cdot \hat{p}_{3\perp}) \right. \\ \left. - i \cos^{-1}(\hat{x}_\perp \cdot \hat{p}_{4\perp}) + \int_{|x_\perp| \parallel p_{3\perp}}^\infty \frac{dt}{t} J_0(t) e^{-i\hat{x}_\perp \cdot \hat{p}_{3\perp} t} + \int_{|x_\perp| \parallel p_{4\perp}}^\infty \frac{dt}{t} J_0(t) e^{i\hat{x}_\perp \cdot \hat{p}_{4\perp} t} \right\}, \quad (38)$$

The dependence on the transverse momenta  $p_{3\perp}$  and  $p_{4\perp}$  in this term arises from the Mandelstam-Leibbrandt prescription for the infrared singularities. This potential is clearly small at large  $x_\perp$ ; however, at small  $x_\perp$  it gives a  $-\ln \mu^2 x_\perp^2$  contribution that precisely cancels the logarithmic term in Eq. (36). Of course, to find the correct short distance form one has to also include the other terms from Eqs. (32) and (35) that were dropped in arriving at Eq. (36).

Finally, a simple choice of  $f$  that satisfies the above conditions is  $f(\Gamma) = \delta(\Gamma - 1) + \delta'(\Gamma - 1)$ . This yields

$$V_{LR}(x^-, x_\perp) = \frac{g_R^2 \mu^2 T^a T^a}{4\pi\rho} \left\{ \frac{2}{2-d} + \gamma + E_1 \left( \frac{\mu^2 x_\perp^2}{4\rho |x^-|} \right) \right. \\ \left. + \ln \left( \frac{\mu^2 x_\perp^2}{4\pi} \right) \right\}, \quad (39)$$

where we have dropped yet another short range piece. Since the divergent constant in Eq. (39) is infrared in nature, it does not get cancelled by a counterterm. This is important. Perry [13] has argued that this divergence is cancelled by a similar infrared divergence in the quark self-energy for color singlet states, but that for color nonsinglet states this cancellation does not occur.

## IV. TOWARD A NONPERTURBATIVE SOLUTION

### A. Dyson-Schwingerish equations

Within the WG and W schemes, there does not seem to be any great advantage in solving for the dressed Hamiltonian by using the perturbative expansion (16). Rather, we can express the dressed Hamiltonian from the outset in terms of normal-ordered products of field operators as follows:

$$H_{I\sigma}(t) = \sum_N h_{\sigma\mathcal{N}}(\{p\}) e^{ip^0 t} \mathcal{N}_{\{p\}} \equiv \sum_N h_{\sigma\mathcal{N}} \mathcal{N}_{\{p\}}(t), \quad (40)$$

The divergent piece in Eq. (36) can be seen to be of infrared nature since it arises from a factor  $\Gamma((d/2) - 1)$ , which is regulated by increasing  $d$ .

We have dropped a short-range term from the potential in going from Eq. (35) to Eq. (36), namely,

where  $p = p^O - p^I$ , as before, and  $\mathcal{N}_{\{p\}}(t) = e^{iH_0 t} \mathcal{N}_{\{p\}} e^{-iH_0 t}$ . Taking the Fourier transform of Eq. (12)—we only consider the W scheme here—we find

$$H_{I\sigma}(t) = \int dt' \tilde{f}(t-t') H_I(t') + \int_\sigma^\infty d\sigma' \\ \times \int dt' dt'' \tilde{F}_{\sigma\sigma'}(t-t'', t''-t') H_{I\sigma'}(t') H_{I\sigma'}(t''), \quad (41)$$

where  $\tilde{f}(t)$  is the Fourier transform of  $f(\omega)$  and

$$\tilde{F}_{\sigma\sigma'}(t_1, t_2) = \int \frac{d\omega}{2\pi} \frac{d\omega'}{2\pi} e^{i\omega t_1} e^{i\omega' t_2} \frac{f\left(\frac{\omega}{\sigma}\right)}{f\left(\frac{\omega}{\sigma'}\right)} \\ \times \left\{ \frac{d_{\sigma'} \ln f\left(\frac{\omega'}{\sigma'}\right)}{\omega'} - \frac{d_{\sigma'} \ln f\left(\frac{\omega - \omega'}{\sigma'}\right)}{\omega - \omega'} \right\}. \quad (42)$$

Now let us choose the similarity function suggested in Sec. II, namely,  $f(x) = (1+x^2)^{-1}$ . Then the term in the brackets in Eq. (42) has a pole structure in  $\omega'$  that yields step functions in  $t_2$  after integration. We find

$$H_{I\sigma}(t) = \frac{\sigma}{2} \int dt' e^{-\sigma|t-t'|} H_I(t') \\ - \frac{i\sigma}{4} \int_\sigma^\infty d\sigma' \frac{\sigma'^2 - \sigma^2}{\sigma'^3} \int dt' dt'' e^{-\sigma'|t'-t''|} \\ \times (e^{-\sigma|t-t'|} + e^{-\sigma|t-t''|}) [\mathcal{T}\{H_{I\sigma'}(t') H_{I\sigma'}(t'')\} \\ - \bar{\mathcal{T}}\{H_{I\sigma'}(t') H_{I\sigma'}(t'')\}], \quad (43)$$

where  $\bar{\mathcal{T}}$  orders in the opposite sense as  $\mathcal{T}$ . When we substitute the expansion (40) in Eq. (43), we find that contractions of field operators resulting from normal-ordering in the right-hand side will only be of the Feynman type. Moreover, we need only consider the operator

$$\begin{aligned} K_\sigma(t) &= \frac{\sigma}{4} \int dt' e^{-\sigma|t-t'|} H_I(t') \\ &\quad - \frac{i\sigma}{4} \int_\sigma^\infty d\sigma' \frac{\sigma'^2 - \sigma^2}{\sigma'^3} \int dt' dt'' e^{-\sigma'|t-t''|} \\ &\quad \times (e^{-\sigma|t-t'|} + e^{-\sigma|t-t''|}) \mathcal{T}\{H_{I\sigma'}(t') H_{I\sigma'}(t'')\}, \end{aligned} \quad (44)$$

since from the hermiticity of  $H_{I\sigma}$  we have

$$H_{I\sigma}(t) = K_\sigma(t) + K_\sigma^\dagger(t). \quad (45)$$

The calculation of  $K_\sigma$  involves only proper Feynman propagators, and one need only consider connected graphs since disconnected graphs will not contribute to  $H_{I\sigma}$  since they are cancelled by identical terms from  $K_\sigma^\dagger$ .

We expand  $K_\sigma(t)$  as we did for  $H_{I\sigma}(t)$  in Eq. (40)—so that  $h_{\sigma\mathcal{N}} = k_{\sigma\mathcal{N}} + k_{\sigma\mathcal{N}}^*$ —and substitute in Eq. (44). The amplitudes  $k_{\sigma\mathcal{N}}$  so defined are to be solved by iteration. One can always organize such an iterative solution to reproduce the perturbative expansion of Sec. III, should one care to. Indeed, by expanding the dressed amplitudes  $h_{\sigma\mathcal{N}}$  in powers of the undressed amplitudes  $h_{\mathcal{N}}$ , one recovers the perturbative scheme of Sec. III A. However, now there are other more interesting possibilities, for just as with Dyson-Schwinger

equations one can use a variety of approximations to Eq. (44) in order to sum up infinite classes of diagrams. We note that Eq. (44) permits a Wick rotation to Euclidean space and thus the normal power counting applies in determining the counterterm structure. This does not seem to be true for all choices of the similarity function  $f$ .

### B. In the Dyson picture

We can also develop Dyson-Schwinger-like equations for the intermediate Hamiltonian by introducing a new time scale  $T > 0$  into the integrals in Eq. (19). We define

$$S_D(t, T) = \mathcal{T}\{e^{-i\int_{t-T}^t dt' H_I(t, t')}\}, \quad (46)$$

so that

$$\begin{aligned} H_I^D(t, T) &= - \int_{t-T}^t dt' d_t H_I(t, t') \\ &\quad + i \int_{t-T}^t dt' [H_I(t, t'), H_I^D(t, t-T)], \end{aligned} \quad (47)$$

which is a linear integral equation. The usual intermediate Hamiltonian is then obtained from  $H_I^D(t, T)$  by taking the limit  $T \rightarrow \infty$ . The solution to Eq. (47) has the form

$$\begin{aligned} H_I^D(t, T) &= \sum_n g_R^n \int_{t-T}^t dt' e^{i\sigma\Lambda_n(t-t')} \sum_{\mathcal{N}} h_{D\mathcal{N}}^{(n)}(\{p\}, \{\Gamma\}) \\ &\quad \times \mathcal{N}_{\{p\}}(t'). \end{aligned} \quad (48)$$

$K_D(t, T)$  is defined analogously to  $K_\sigma(t)$  above, and we find

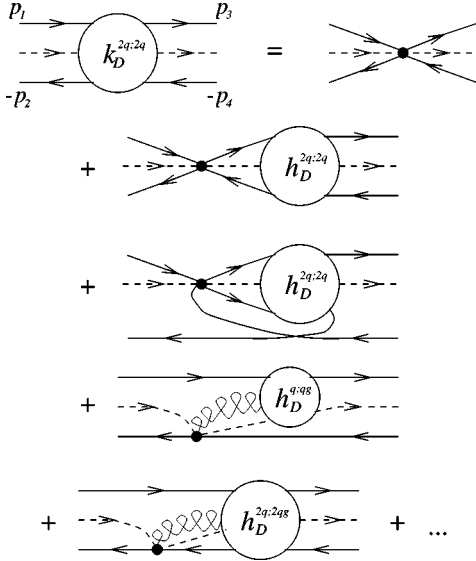
$$\begin{aligned} K_D(t, T) &= \sum_n g_R^n \int_{t-T}^t dt_0 e^{i\Lambda_n(t-t_0)} \sum_{\mathcal{N}} k_{D\mathcal{N}}^{(n)} \mathcal{N}_{\{p\}}(t_0) \\ &= \sum_n g_R^n \int_{t-T}^t dt_0 e^{i\Lambda_n t} \left\{ \frac{\sigma n \Gamma_1}{2} e^{-i\Lambda_n t_0} \sum_{\mathcal{N}} h_{\mathcal{N}}^{(n)} \mathcal{N}_{\{p\}}(t_0) \right. \\ &\quad \left. + i \sum_{n'=1}^n \int_{t_0}^t dt_1 e^{-i(\Lambda_n - \Lambda_{n'})t_0} e^{-i\sigma\Lambda_{n'}t_1} \sum_{\mathcal{N}\mathcal{N}'} h_{\mathcal{N}}^{(n-n')} h_{D\mathcal{N}'}^{(n')} \mathcal{T}(\mathcal{N}_{\{p\}}(t_0) \mathcal{N}_{\{p'\}}(t_1)) \right\}. \end{aligned} \quad (49)$$

The time-ordered product is expanded using Wick's theorem and the product of all contractions—that is, the product of  $N_q$  boson and fermion propagators—is written as  $\mathcal{M}_{\{q\}}$ , so that we have

$$\mathcal{T}\{\mathcal{N}_{\{p\}}(t) \mathcal{N}_{\{p'\}}(t')\} = \delta_{N_q N_{q'}} \left\{ \prod_{i=1}^{N_q} (2\pi)^4 \delta^{(4)}(q'_i - q_i) \right\} \mathcal{M}_{\{q\}} : \mathcal{N}_{\{p/q\}}(t) \mathcal{N}_{\{p'/q'\}}(t') :. \quad (50)$$

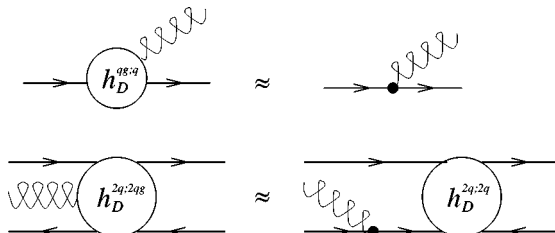
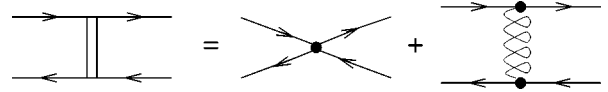
The notation  $\mathcal{N}_{\{p/q\}}$  means the  $N_q$  field operators corresponding to the contractions are dropped from the normal-ordered product  $\mathcal{N}_{\{p\}}$ . We now take the limit  $T \rightarrow \infty$ , express the step functions limiting the time integrals as complex integrations as in the previous section, and then perform the time-integrals in Eq. (49). Then using Eq. (50), the amplitudes satisfy

$$\begin{aligned} k_{D\mathcal{N}}^{(n)} 2\pi \delta(p - \Lambda_n + \Lambda) &= - \frac{i\Lambda_n}{2} h_{\mathcal{N}}^{(n)} 2\pi \delta(p - \Lambda_n + \Lambda) + \sum_{n'=1}^n \int \frac{d\nu'}{2\pi} \frac{1}{\nu' - i\varepsilon} \sum_{\mathcal{N}'\mathcal{N}''} h_{\mathcal{N}'}^{(n-n')} 2\pi \delta(p' - \Lambda_n + \Lambda_{n'} + \Lambda') \\ &\quad \times \mathcal{M}_{\{q\}} h_{D\mathcal{N}''}^{(n')} 2\pi \delta(p - p' - \Lambda_{n'} - \Lambda' + \Lambda), \end{aligned} \quad (51)$$

FIG. 4. Diagrammatic equation for general  $q\bar{q} \rightarrow q\bar{q}$  vertex.

where the last sum is over  $\mathcal{N}, \mathcal{N}'' = \mathcal{N}_{\{p'\}}, \mathcal{N}_{\{p''\}}$  such that  $:\mathcal{N}_{\{p'/q\}}\mathcal{N}_{\{p''/q\}} := \mathcal{N}_{\{p\}}$  and the other quantities are defined as above, with  $\Lambda' = -\nu'\lambda$ . This equation has a simple graphical interpretation in analogy with the spurion diagrams of Sec. III C. If we draw a spurion line as in Fig. 4, entering the undressed vertex with momentum  $\Lambda_n$ , carrying momentum  $\Lambda_{n'} + \Lambda'$  from the undressed to the dressed vertex and exiting the last vertex with momentum  $\Lambda$ , then the total 4-momentum is conserved at each vertex.

Figure 4 is a graphical representation of Eq. (51) for the  $q\bar{q} \rightarrow q\bar{q}$  amplitude. Undressed vertices are denoted by a dot, and dressed vertices (of type  $k_D$  or  $h_D$ ) are denoted by a bubble. The resemblance to Dyson-Schwinger equations is evident. The dots indicate that we have not shown diagrams that modify the quark legs only (counterterm diagrams from the undressed Hamiltonian and  $\sigma$ -dependent mass terms from the dressed Hamiltonian) as well as diagrams that involve dressed vertices with more than five total quark and gluon legs. The diagrams for  $k_D^\dagger$  are equivalent to those shown here, except the direction of the spurion line is reversed. Diagrammatically, it is easy to see how an iterative solution of these equations, starting with the undressed vertices as input, will reproduce the perturbative diagrams of Sec. III C. Of course, the diagrams are precisely equivalent only in the limit  $T \rightarrow \infty$ . Note finally that because the amplitude  $k_D^{2q;2q}(p_3, -p_2; -p_4, p_1)$  enters  $K_D$  as the coefficient

FIG. 5. Approximations for  $q \rightarrow qg$  and  $q\bar{q}g \rightarrow q\bar{q}$  vertices.FIG. 6. Definition of input potential for approximation to  $q\bar{q} \rightarrow q\bar{q}$  vertex.

of  $:\psi^\dagger(p_3)\psi^\dagger(-p_2)\psi(-p_4)\psi(p_1):$ , which is antisymmetric under either  $p_1 \leftrightarrow -p_4$  or  $p_3 \leftrightarrow -p_2$  and symmetric under  $(p_1, -p_4) \leftrightarrow (p_3, -p_2)$  plus complex conjugation, the diagrams in Fig. 4 represent additional processes—for example, the last diagram shown represents processes where the undressed  $qg \rightarrow q$  vertex is attached to any of the four quark legs.

An advantage to having an equation that is linear in the dressed vertices, as in the present case, is that the undressed Hamiltonian has a finite number of terms, whereas the dressed Hamiltonian can have terms with any number of legs. Thus a diagrammatic expansion for any given dressed vertex based upon Eq. (44), which is nonlinear in the dressed vertices, will contain an infinite number of graphs since there can be any number of internal lines connecting the two dressed vertices. In contrast, the diagrammatic expansion for any given dressed vertex based upon Eq. (51) contains a finite number of graphs, since the number of internal lines is limited by the undressed vertices.

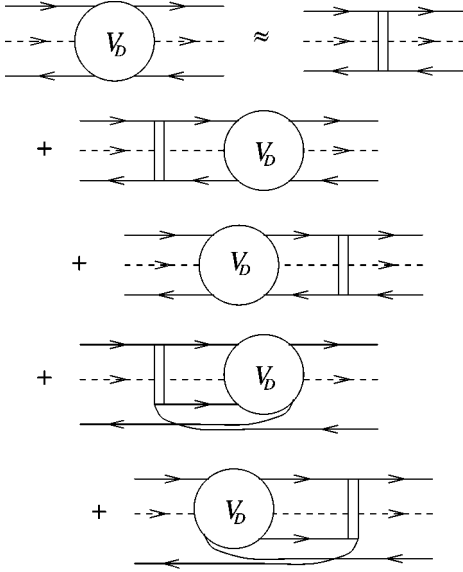
### C. Ladder summation of LFQCD potential

As an example of this final formulation of the similarity transformation, let us set up the calculation of an approximation to the general quark-antiquark potential in light-front QCD. We start from the diagrams in Fig. 4. There will be similar diagrammatic equations for the dressed  $qg \rightarrow q$  and  $\bar{q}qg \rightarrow \bar{q}q$  that appear in the equation for the dressed  $\bar{q}q \rightarrow \bar{q}q$  amplitude. We may approximate these latter equations as shown in Fig. 5. According to this approximation, we treat perturbatively vertices that change gluon number; in the first approximation the dressed  $q \rightarrow qg$  is equivalent to the undressed vertex. Consistent with this approximation, we take the amplitude  $\bar{q}qg \rightarrow \bar{q}q$  to be as in Fig. 5. This corresponds to taking the input potential for the dressed  $\bar{q}q \rightarrow \bar{q}q$  amplitude to be as in Fig. 6. This yields the  $\mathcal{O}(g_R^2)$  potential calculated in Sec. III D. (For simplicity, we have neglected to draw the spurion lines in Figs. 5 and 6.) The equation for the dressed  $\bar{q}q \rightarrow \bar{q}q$  vertex in this approximation is shown in Fig. 7. This looks very much like the Bethe-Salpeter equation. Here again, we have ignored corrections to the external legs. Clearly, improving the approximations for the gluon-number-changing vertices corresponds to including higher-order radiative corrections to the input potential of Fig. 6.

While we shall not solve for this dressed amplitude here, it is perhaps instructive to set up the equations in some detail. From the above, the dressed vertices are

$$h_{DN}^{(n)}(t) = e^{ip^0 t} \int \frac{dv}{2\pi i} \frac{1}{v - i\varepsilon} h_{DN}^{(n)}(\Lambda) \quad (52)$$

with  $h_{DN}^{(n)}(\Lambda) \equiv 2\pi\delta(p - \Lambda_n + \Lambda)h_{DN}^{(n)}$  satisfying

FIG. 7. Bethe-Salpeter-like approximation to  $q\bar{q} \rightarrow q\bar{q}$  vertex.

$$\begin{aligned}
h_{D\Lambda}^{(n)}(\Lambda) &= -i\Lambda_n h_{\Lambda'}^{(n)}(\Lambda) + \sum_{n'=1}^n \int \frac{d\nu'}{2\pi} \sum_{\Lambda''\Lambda'''} \frac{1}{\nu' - i\epsilon} \\
&\times h_{\Lambda''}^{(n-n')}(\Lambda') \mathcal{M}_{\{q\}} h_{D\Lambda'''}^{(n')}(\Lambda - \Lambda') \\
&- \sum_{n'=1}^n \int \frac{d\nu'}{2\pi} \sum_{\Lambda''\Lambda'''} \frac{1}{\nu - \nu' - i\epsilon} \\
&\times h_{D\Lambda''}^{(n-n')}(\Lambda') \mathcal{M}_{\{q\}} h_{\Lambda'''}^{(n')}(\Lambda - \Lambda'). \quad (53)
\end{aligned}$$

Let us call the dressed  $q\bar{q} \rightarrow q\bar{q}$  vertex  $h_{1D}^{2q;2q} \equiv V_D$ ; the dressed  $q \rightarrow qg$  vertex  $h_{1D}^{qg;q} \equiv \phi_D$ ; and the dressed  $q\bar{q}g \rightarrow q\bar{q}$  vertex  $h_{1D}^{2qg;2q} \equiv \Psi_D$ . Undressed vertices, as above, are denoted by dropping the subscript  $D$ —note that  $\Psi = 0$ . Now the approximations of Fig. 5 are

$$\phi_D^{(n)}(\Lambda) \sim \delta^{n1} \sigma \Gamma_1 \phi^{(1)}(\Lambda); \quad (54)$$

$$\begin{aligned}
\Psi_D^{(n+1)}(\Lambda) &\sim \int \frac{d\nu'}{2\pi} \int \frac{d^4q}{(2\pi)^4} \left\{ \frac{1}{\nu' - i\epsilon} \phi^{(1)}(\Lambda') iS_F(q) \right. \\
&\times V_D^{(n)}(\Lambda - \Lambda') - \frac{1}{\nu - \nu' - i\epsilon} V_D^{(n)}(\Lambda') iS_F(q) \\
&\left. \times \phi^{(1)}(\Lambda - \Lambda') \right\}. \quad (55)
\end{aligned}$$

The undressed  $\mathcal{O}(g_R)$  quark-gluon vertex is [9]

$$\begin{aligned}
g_R \phi^{(1)}(\Gamma) &= \phi(p_3, q; p_1) (2\pi)^4 \delta(p_3 + q - p_1 - \Lambda_1 + \Lambda), \\
\phi(p_3, q; p_1) &= -g_R T^a \left\{ 2 \frac{q_\perp^i}{[q^+]} - \frac{\sigma_\perp \cdot p_{3\perp} - im_F}{[p_3^+]} \sigma_\perp^i \right. \\
&\quad \left. - \sigma_\perp^i \frac{\sigma_\perp \cdot p_{1\perp} + im_F}{[p_1^+]} \right\}. \quad (56)
\end{aligned}$$

The undressed  $\mathcal{O}(g_R^2) q\bar{q} \rightarrow q\bar{q}$  vertex is

$$\begin{aligned}
g_R^2 V^{(2)}(\Lambda) &= V(p_3 - p_1) (2\pi)^4 \delta(p_3 + p_4 - p_1 - p_2 - \Lambda_2 + \Lambda) \\
V(p_3 - p_1) &= 4g_R^2 T^a T^a \frac{1}{[p_3^+ - p_1^+]^2}. \quad (57)
\end{aligned}$$

We have seen these undressed vertices in the perturbative calculation of Sec. III D.

The next to the last graph in Fig. 4 is

$$\int \frac{d\nu'}{2\pi} \frac{1}{\nu' - i\epsilon} \int \frac{d^4q}{(2\pi)^4} \phi^\dagger(\Lambda') iD_F(q) \phi_D(\Lambda - \Lambda'). \quad (58)$$

Using the approximation (54), this becomes

$$\begin{aligned}
V_c(\Lambda) &\equiv - \int \frac{d\nu'}{2\pi i} \frac{\sigma \Gamma_1}{\nu' - i\epsilon} \phi^\dagger(-p_2, \tilde{q}; -p_4) D(\tilde{q}) \\
&\times \phi(p_3, -\tilde{q}; p_1) (2\pi)^4 \delta(p - \Lambda_2 + \Lambda), \quad (59)
\end{aligned}$$

where  $\tilde{q} = p_2 - p_4 + (i\Gamma_2 + \nu')\lambda$ . There is a similar contribution to  $\Phi$  from the term  $k_{1D}^\dagger$ . Indeed, it is identical after the replacement  $\tilde{q} \rightarrow q = p_3 - p_1 - (i\Gamma_2 + \nu')\lambda$ —this corresponds to reversing the direction of the spurion line. We write this as  $V_c = V_b|_{q \rightarrow \tilde{q}}$ , as in Sec. III D. After integration over  $\nu'$ , the sum of these terms and the undressed vertex  $V$  gives the input potential of Fig. 6, namely,

$$\begin{aligned}
V_0(\Lambda) &= 2\sigma \Gamma_1 V(\Lambda) + V_b(\Lambda) + V_c(\Lambda) \\
&= \sigma \Gamma_1 V_0 (2\pi)^4 \delta(p - \Lambda_2 + \Lambda), \quad (60)
\end{aligned}$$

where

$$\begin{aligned}
V_0(p_3, -p_2; -p_4, p_1) &= V(q) + V(\tilde{q}) \\
&- \phi^\dagger(-p_2, q; -p_4) D(q) \phi(p_3, -q; p_1) - \phi^\dagger(-p_2, \tilde{q}; -p_4) D(\tilde{q}) \phi(p_3, \tilde{q}; p_1), \quad (61)
\end{aligned}$$

with  $q = p_3 - p_1 - i\Gamma_2\lambda$  and  $\tilde{q} = p_2 - p_4 + i\Gamma_2\lambda$ . Substituting this into Eq. (52), we recover the order  $g_R^2$  potential of Sec. III D, as indeed we must. Thus the first and fourth terms on the right-hand side of the equation in Fig. 4 plus their conjugate graphs sum to give the first term on the right-hand side in Fig. 7.

The last graph in Fig. 4 is

$$-\int \frac{d\nu''}{2\pi i} \int \frac{d^4 q''}{(2\pi)^4} \frac{1}{\nu'' - \nu' - i\epsilon} \phi^\dagger(-p_2, q; -q'; \Lambda') D(q) S_F(-q') \times \phi(q'', -q; p_1; \Lambda'' - \Lambda') S_F(q'') V_D(p_3, -q'; -p_4, q''; \Lambda - \Lambda''), \quad (62)$$

plus a similar term in which the gluon couples leg  $-p_2$  to  $p_3$ . Other terms are either ignored because they only correct the external legs or else not distinct because of the symmetries of the amplitude. The term given in Eq. (63) may be summed with the second graph on the right-hand side of the equation in Fig. 4 to give

$$V_0(q, -p_2; -q', p_1; \Lambda') S_F(q) S_F(-q') \Phi_D(p_3, -q'; -p_4, q; \Lambda - \Lambda'). \quad (63)$$

This is the second graph on the right-hand side in Fig. 7. The remaining graphs in Fig. 7 result from Eq. (64) by complex conjugation (reversing the spurion line) and by the substitution  $-p_2 \leftrightarrow -p_4$ . We have, finally,

$$\begin{aligned} V_D(p_3, -p_2; -p_4, p_1; \Lambda) = & V_0(p_3, -p_2; -p_4, p_1; \Lambda) + \int \frac{d\nu'}{2\pi} \int \frac{d^4 q}{(2\pi)^4} \int \frac{d^4 q'}{(2\pi)^4} \\ & \times \left\{ V_0(q, -p_2; -q', p_1; \Lambda') \frac{S_F(q) S_F(-q')}{\nu' - i\epsilon} V_D(p_3, -q'; -p_4, q; \Lambda - \Lambda') \right. \\ & + V_D(q, -p_2; -q', p_1; \Lambda') \frac{S_F(q) S_F(-q')}{\nu - \nu' - i\epsilon} V_0(p_3, -q'; -p_4, q; \Lambda - \Lambda') \\ & - V_0(q, q'; p_4, p_1; \Lambda') \frac{S_F(q) S_F(q')}{\nu' - i\epsilon} V_D(p_3, p_2; q', q; \Lambda - \Lambda') \\ & \left. - V_D(q, q'; p_4, p_1; \Lambda') \frac{S_F(q) S_F(q')}{\nu - \nu' - i\epsilon} V_0(p_3, p_2; q', q; \Lambda - \Lambda') \right\}. \quad (64) \end{aligned}$$

It would be interesting to approximate  $V_0$  further by just taking the long range (small  $\bar{q}$ ) part calculated in Sec. III D and substituting this in Eq. (65). The infrared divergence in  $V_0$  will be cancelled by divergences in the self-energy corrections to the external legs (see Sec. III D)—corrections which we have ignored here but which must be included if one wants to solve this Bethe-Salpeter-like equation in a consistent manner. This paper is long enough already, and therefore such a calculation will not be undertaken here.

## V. CLOSING ARGUMENTS

In this paper we have developed a similarity renormalization framework for the study of strongly interacting field theories. The basic view of this approach is that Hamiltonian methods will prove most fruitful for the solution of such theories. The generic theory for which our framework has been developed has interactions that are weak asymptotically but grow large enough at low energy to invalidate perturba-

$$\int \frac{d\nu'}{2\pi} \frac{1}{\nu' - i\epsilon} \int \frac{d^4 q}{(2\pi)^4} \int \frac{d^4 q'}{(2\pi)^4} \times \phi^\dagger(\Lambda') D(q) S_F(-q') \Psi(\Lambda - \Lambda'). \quad (62)$$

Using the approximation (55), the integrand in Eq. (62) becomes

tion theory. QCD is of course the theory that we particularly have in mind. The basic idea behind the similarity renormalization scheme is that the Hamiltonian of such a theory can be transformed into that of an effective many-body theory where states that differ greatly in free energy are essentially uncoupled. This resulting many-body Hamiltonian can then be solved with recourse to the many available approximate methods such as variational approaches, trial wave functions, iterative techniques, and numerical basis function approaches. The similarity transformation achieves this goal by smoothly eliminating interactions between states whose free energies differ by an amount greater than an arbitrary scale  $\sigma$  introduced by the transformation. The result of this elimination is to create new interactions between states that differ in energy by an amount less than  $\sigma$ . The assumption is that from these new interactions one can extract potentials that describe the relevant physics.

Clearly, no physical result can depend on the renormalization scale  $\sigma$ . However, the calculations can only be ap-

proximately carried out for most systems of interest, and so one will need to choose a value of  $\sigma$  that makes the approximations as valid as possible. Computations in this framework involve two steps: first, the similarity transformed Hamiltonian is calculated; second, this Hamiltonian is solved. The first step is most easily done perturbatively, which requires that  $\sigma$  be large since only at high energy is the coupling small (by assumption). The second step is most easily done when as few states as possible are coupled strongly, which requires that  $\sigma$  be as small as possible. Inevitably, one must make a compromise and choose  $\sigma$  in some intermediate range. If the Dyson-Schwinger-like equations developed in the last section can be implemented, it may be possible to go beyond the perturbative calculation of the dressed Hamiltonian so that  $\sigma$  can be lowered to values for which perturbation theory begins to break down. However, in most cases it will probably be better to keep  $\sigma$  large enough that the Hamiltonian can be dressed perturbatively, since the tools available for the second step are generally more powerful.

That the elimination of couplings between states separated by large energy differences turns a field theory into a many-body theory is clear if the free particles are massive. If  $\sigma$  is lowered to just above the particle masses, then creating or destroying a particle will cause an energy difference of order  $\sigma$ . This means interactions that change particle number will be suppressed. If the particles are light or massless, however, as in QCD, it does not follow that the similarity transformation described here will suppress interactions that change particle number. Indeed, one might consider it better to have the similarity function depend on differences in particle number rather than on differences in energy. However, such a transformation is unlikely to be feasible in perturbation theory, for one no longer has a means of eliminating only high energy degrees of freedom. Moreover, one would lose the advantage that small energy denominators are avoided. Instead, one can use the similarity transformation in a light-front formulation of a theory such as QCD. We shall argue in the following that this change of formulation of the theory will provide a means of turning even QCD into a many-body problem.

The use of light-front coordinates in field theory is not new (see Ref. [3] for a review and an exhausting—if perhaps not quite exhaustive—list of references). Such calculations are considered difficult, partly because they are unfamiliar, but also because they really are difficult. One of the major difficulties with the use of light-front coordinates is that Lorentz covariance is no longer manifest once one chooses a particular direction in defining the light-front time. Another problem is that calculations are only feasible for a particular gauge choice, the light-cone gauge. These problems severely complicate the renormalization of divergences, and this has slowed the advance in light-front computations. The fact that in our similarity renormalization scheme the calculation of the dressed Hamiltonian can be expressed in terms of Feynman diagrams is therefore significant. It means that divergences can be handled with dimensional regularization, the infrared singularities can be handled with the Mandelstam-Leibbrandt prescription, and the counterterm structure is then that of covariant formulations (with noncovariant gauges). In

particular, renormalization of divergences for QCD in equal-time coordinates and the light-cone gauge is well understood (see, for example, Refs. [10,11]), and we can rely on such prior work in determining the dressed Hamiltonian in the intermediate representation. There are of course other, more technical difficulties resulting from the choice of light-front coordinates (for example, rotations about the transverse axes are no longer kinematical); but these should not be prohibitive. Indeed, there are also some technical advantages to the use of light-front as compared to equal-time coordinates (for example, now boosts are kinematical).

The essential reasons for using light-front coordinates follow from the free particle dispersion relation

$$p^- = \frac{p_\perp^2 + m^2}{p^+}. \quad (66)$$

This implies that all on-shell particles (and antiparticles) have longitudinal momentum  $p^+ \geq 0$  and all physical states have total longitudinal momentum  $P^+ \geq 0$ . The vacuum has  $P^+ = 0$  and is therefore built only from particles with  $p^+ = 0$ . From Eq. (66) we see that such particles have infinite (light-front) energy unless  $p_\perp^2 = 0$  and  $m^2 = 0$ . The similarity transformation will decouple the infinite energy states from the low-energy physics, and the computation of the vacuum state is then greatly simplified. Indeed, if we give gluons a small mass, all particles with  $p^+ = 0$  have infinite energy, and the vacuum state of the dressed Hamiltonian is just the trivial free vacuum state. Likewise, in building any bound state of the dressed Hamiltonian, we can rely on the fact that the total longitudinal momentum  $P^+$  must be built up from constituent longitudinal momenta  $p_i^+ \geq 0$ . If the energy of each constituent is to be less than  $\sigma$ , we must have  $p_i^+ \geq (p_{\perp i}^2 + m^2)/\sigma$  for all  $p_i^+$ , and thus in effect we have a bound on the number of particles that can make up a state. Again, the only particles that escape this lower bound on the longitudinal momentum are (massless) gluons with  $p_{\perp i}^2 \sim 0$ , but one can hope that such highly transversely localized particles will have little contribution to low-energy states. In any case, it is clear that effects associated with the quark-gluon sea in the equal-time formulation of QCD will be largely, if not totally, replaced by interactions in the dressed Hamiltonian after a similarity transformation in the light-front formulation.

But the most interesting result of the light-front formulation is that longitudinal and transverse variables scale differently (this has been repeatedly emphasized by Wilson [19]). This can be seen from the dispersion relation (66) and has been discussed in Sec. III D. Thus the similarity renormalization of light-front Hamiltonians depends on the energy scale  $\sigma$  through both a mass scale  $\mu$  and a longitudinal momentum scale  $\rho$ . The mass scale  $\mu$  may be taken to be that introduced by dimensional regularization. The QCD coupling  $g_R$  runs with this scale, and  $\mu$  must be taken large to keep  $g_R$  small enough for perturbation theory to remain valid. However, the similarity function  $f$  runs with the ratio  $\sigma = \mu^2/\rho$ ; and thus, even though the mass scale  $\mu$  be large, we can suppress couplings between states with energy differences above a

given value by making the longitudinal scale  $\rho$  large enough. We have seen that light-front energy increases with particle number; and therefore at large  $\rho$  the similarity transformation will suppress number changing interactions in the dressed Hamiltonian, thus turning the solution of QCD bound states into a many-body problem. If the quarks and gluons are assigned large constituent masses—and this is a perfectly valid choice [3] at second order in the similarity renormalization scheme—then the many-body problem is indeed a few-body problem. That the mass scale  $\mu$  may be nevertheless kept large provides the possibility that the transformation may be accurately calculated in perturbation theory. That Dyson's intermediate representation is a particular similarity renormalization scheme that may be expressed in terms of ordi-

nary Feynman graphs means that perturbative light-front QCD computations are feasible. These computations should yield a dressed Hamiltonian that is considerably closer to strong-interaction phenomenology than the usual free QCD Hamiltonian. That we find a confining potential already at tree level may be taken as a positive indication of the utility of this approach.

#### ACKNOWLEDGMENTS

I have benefited from past discussions with Ken Wilson, Avaroth Harindrinath, and Robert Perry. I thank J. S. Walhout for first pointing out Ref. [6] to me.

- 
- [1] K. G. Wilson, Phys. Rev. **140**, B445 (1965).  
 [2] St.D. Głazek and K. G. Wilson, Phys. Rev. D **48**, 5863 (1993); **49**, 4214 (1994).  
 [3] K. G. Wilson, T. S. Walhout, A. Harindranath, W. M. Zhang, R. J. Perry, and St. D. Głazek, Phys. Rev. D **49**, 6720 (1994).  
 [4] K. Wegner, Ann. Phys. (N.Y.) **3**, 77 (1994).  
 [5] F. J. Dyson, Phys. Rev. **82**, 428 (1951); **83**, 608 (1951); **83**, 1207 (1951); Proc. R. Soc. London **A207**, 395 (1951).  
 [6] For a brief historical account of Dyson's papers, see S. S. Schweber, *QED and the Men Who Made It: Dyson, Feynman, Schwinger, and Tomonaga* (Princeton University Press, Princeton, 1994), pp. 556–565.  
 [7] V. G. Kadashevsky, Sov. Phys. JETP **19**, 443 (1964); **19**, 597 (1964); Nucl. Phys. **B6**, 125 (1968).  
 [8] For a review, with emphasis on a light-front formulation, see V. A. Karmanov, Sov. J. Part. Nucl. **19**, 228 (1988).  
 [9] W.-M. Zhang and A. Harindranath, Phys. Rev. D **48**, 4881 (1993).  
 [10] A. Bassetto, M. Dalbasco, and R. Soldati, Phys. Rev. D **36**, 3138 (1987).  
 [11] A. Bassetto, G. Nardelli, and R. Soldati, *Yang-Mills Theories in Algebraic Non-Covariant Gauges* (World Scientific, Singapore, 1991).  
 [12] H. C. Lee and M. S. Milgram, Nucl. Phys. **B268**, 543 (1986).  
 [13] R. J. Perry, in *Hadron Physics 94*, edited by V. E. Herscovitz and C. Vasconcellos (World Scientific, Singapore, 1995); and in *Theory of Hadrons and Light-Front QCD*, edited by St. D. Głazek (World Scientific, Singapore, 1994), pp. 56–70.  
 [14] W.-M. Zhang, Phys. Rev. D **56**, 1528 (1997).  
 [15] St. D. Głazek, Acta Phys. Pol. B **29**, 1979 (1998).  
 [16] K. G. Wilson and D. R. Robertson, in *Theory of Hadrons and Light-Front QCD* (Ref. [13]), pp. 15–28.  
 [17] S. Mandelstam, Nucl. Phys. **B213**, 718 (1983); G. Leibbrandt, Phys. Rev. D **29**, 1699 (1984).  
 [18] See, for example, R. Soldati, in *Theory of Hadrons and Light-Front QCD* (Ref. [16]), pp. 193–197.  
 [19] K. G. Wilson, OSU internal reports, 1989, 1990, 1993 (unpublished); (private communication).